Role of Chromosomal Microarray and RNA Fusion Analysis in Detecting KMT2A Partial Tandem Duplication with High Mortality in Myeloid Neoplasms: A Retrospective Study

Bhaumik Shah, MD[1], Jianming Pei, MD[1], Roniya Francis, MD[1], Peter Abdelmessieh, MD[2], Mariusz Wasik, MD[1], Nicholas Mackrides, MD[1], Reza Nejati, MD[1]

[1]Department of Pathology, Fox Chase Cancer Center, Temple Health, Philadelphia, Pennsylvania, USA

[2]Department of Bone Marrow Transplant & Cellular Therapy, Fox Chase Cancer Center, Temple Health, Philadelphia, Pennsylvania, USA

≠ Correspondence: Reza Nejati, Department of Pathology, Fox Chase Cancer Center, Temple University Health System, 333 Cottman Avenue, Philadelphia, PA 19111; email: Reza.Nejati@fccc.edu.

Abstract

KMT2A partial tandem duplication (PTD) is a recurrent genetic alteration in myeloid neoplasms, conferring poor prognosis. *KMT2A*-PTDs are complex gene rearrangements that cannot be fully ascertained using a single genomic platform. There is no universally accepted gold standard for detecting *KMT2A*-PTDs due to the technical limitations of individual methods and the genomic complexity of PTDs. A retrospective analysis was performed at Fox Chase Cancer Center to compare the utility of chromosomal microarray (CMA; Affymetrix CytoScan HD, 2,696,168 markers) and RNA fusion analysis (Illumina TruSight 523-gene RNA Fusion Panel) in 97 specimens (79 bone marrow, 18 peripheral blood) from 17 patients (12 males, 5 females; median age 68 years) with *KMT2A*-PTD-positive myeloid neoplasms (11 AML, 4 MDS, 2 MPN), diagnosed between January 2011 and February 2025. A total of 31 specimens were confirmed as *KMT2A*-PTD-positive by chromosomal microarray (CMA; n = 24) or RNA fusion panel (n = 21). The 73.3% overall concordance (κ = 0.467) between CMA and RNA fusion, with 45.2% *KMT2A*-PTD-specific concordance, underscores their complementary roles. RNA fusion demonstrated superiority in discordant cases (p = 0.035), reflecting its sensitivity for cryptic PTDs, while CMA identified non-canonical PTDs (e.g., Patient 16) and secondary genomic abnormalities (e.g., trisomy 8, CN-LOH in patient 14). The KMT2A-PTD-positive group exhibited greater genomic complexity, with 17 secondary chromosomal abnormality types compared to 6 in the PTD-negative group, reflecting increased clonal heterogeneity. RNA fusion analysis revealed significantly higher median split reads (p = 0.032) and split read-to-coverage (SR/C) ratios (p = 0.046), suggesting elevated *KMT2A*-PTD transcript expression in CMA *KMT2A*-PTD(+) patients lacking additional chromosomal abnormalities (vs. CMA *KMT2A*-PTD (−) patients with abnormalities, p = 0.014-0.020). This may reflect purer PTD clones or fewer competing genomic events. Chromosomal microarray analysis (CMA) identified genomic coverage of *KMT2A* exons 2-20 (except in patient 16). RNA fusion analysis showed consistent breakpoints between exon 10 and exon 2 (16,200 bp) and between exon 11 and exon 2 (13,720 bp). These disruptions affect critical *KMT2A* oncogenic domains: CXXC, PHD, and Bromodomain. Targeted 275-gene DNA-sequencing NGS panel analysis (n=60/97 specimens) revealed specific mutational profiles: *DNMT3A* (51.67%), *TET2* (30.00%), *ASXL1* (21.67%), *RUNX1* (41.67%), *GATA2* (15.00%), *JAK2* (25.00%), *FLT3* (13.33%), *NRAS* (20.00%), *PIK3CA* (11.67%), *EZH2* (18.33%), and *KMT2A* (13.33%). RNA fusion analysis revealed significantly higher median split reads and SR/C ratio of *KMT2A*-PTD in specimens with *DNMT3A* (p ≈

0.0423, 0.0387), *RUNX1* ($p \approx 0.0198$, 0.0234), and *FLT3* ($p \approx 0.0087$, 0.0123). Similarly, significant correlations with RUNX1T1 gain ($p \approx 0.0345$, 0.0412) and cnLOH ($p \approx 0.0214$, 0.0178) indicate higher PTD expression with *RUNX1T1* gain and lower expression with cnLOH.

Kaplan-Meier analysis estimated 41.2% 6-month overall survival (OS). Hematopoietic stem cell transplantation (HSCT) improved outcomes (68.6% vs. 0% OS at 17 months, $p = 0.028$). Non-transplanted patients (10/17, 8 deceased) had a median survival of 6 months. Abnormal karyotypes and FISH-detected *KMT2A* gains were associated with high-risk profiles. Concurrent *FLT3* mutations correlated with 100% mortality ($p=0.0456$). CMA and RNA fusion analysis are complementary, with RNA fusion excelling for cryptic PTDs and CMA for genomic alterations. Optimal management of myeloid neoplasms harboring *KMT2A*-PTD is achieved through the integration of combined testing methodologies, next-generation sequencing, and hematopoietic stem cell transplantation.

Introduction

KMT2A partial tandem duplication (PTD) is a recurrent genetic alteration in myeloid neoplasms, affecting 5-10% of acute myeloid leukemia (AML), 2–7% of myelodysplastic syndromes (MDS), and rarely myeloproliferative neoplasms (MPN) [1, 2]. This structural variant, typically spanning 10-50 kb, involves in-frame duplication of KMT2A exons (e.g., 2-8 or 2-10) via Alu-element-mediated homologous recombination, disrupting the *KMT2A* histone methyltransferase's CXXC and PHD domains[1] . The resultant aberrant protein drives leukemogenesis by upregulating HOX genes, promoting proliferation and differentiation arrest[3]. Approximately 16% of cases develop secondary genomic events, such as copy-neutral loss of heterozygosity (CN-LOH) or PTD allele amplification, enhancing RNA expression and disease progression. *KMT2A*-PTD frequently co-occurs with mutations in *DNMT3A*, *RUNX1*, and *FLT3*, amplifying epigenetic and signaling dysregulation, increasing AML transformation risk from MDS/MPN, and elevating relapse rates [4, 5] . Clinically, *KMT2A*-PTD is associated with poor prognosis, with median overall survival (OS) of 9.85 months in MDS and 4.5–12.1 months in AML, driven by chemoresistance and relapse[4, 6]. It serves as a biomarker for menin inhibitors, targeting the menin-KMT2A interaction, offering a novel therapeutic avenue.

Detecting *KMT2A*-PTD is challenging due to its small size, below the resolution of karyotyping (5–10 Mb) or standard FISH *KMT2A* break-apart probes[7]. Furthermore, its intragenic nature leads to significant overlap in interphase nuclei making its detection unreliable even with custom probe sets targeting the PTD region. Routine NGS panels, optimized for short nucleotide variants, have poor coverage for usual intronic breakpoints of *KMT2A*-PTD and require custom pipelines for structural variant detection. *KMT2A*-PTDs are complex gene rearrangements that cannot be fully ascertained using a single genomic platform. Several methods, including chromosomal microarray (CMA), RNA fusion analysis (e.g., Illumina TruSight RNA Fusion Panel), multiplex ligation-dependent probe amplification (MLPA), next-generation sequencing (NGS), and reverse transcription PCR (RT-PCR), are used, each with strengths and limitations **(Supplemental Table 1).** Historically, long-range RT-qPCR was the gold standard, targeting canonical PTDs (exons 2–8 or 2–10) by amplifying cDNA to detect fusion transcripts [2].

However, hybrid capture NGS (e.g., Oncomine Myeloid Assay) is emerging as the gold standard, detecting PTDs and co-mutations at 10% variant allele fraction (VAF), but is not universally available. Chromosomal microarray (CMA) offers an alternative by detecting copy-number variations (CNVs) and copy-neutral loss of heterozygosity (cnLOH), which are prognostic in AML and MDS, but its sensitivity for intragenic duplications without CNVs is limited [7]. RNA fusion panels, leveraging split-read analysis, detect fusion transcripts with high sensitivity, even in cases with low RNA quality, making them valuable for residual disease monitoring [5]. Optical genome mapping (OGM) can resolve large structural variants, such as 11q gains associated with *KMT2A*-PTD, but is less sensitive for small duplications [7]. Hybrid capture next-generation sequencing (NGS), such as the Oncomine Myeloid Assay, has emerged as the gold standard, detecting PTDs, co-mutations, and allelic complexity at 10% variant allele fraction (VAF) in CAP/CLIA-certified labs [2].

No prior studies have directly compared CMA and RNA fusion panels for *KMT2A*-PTD detection, a critical gap given their complementary strengths. This retrospective study of 97 specimens across 17 patients with *KMT2A*-PTD-positive myeloid neoplasms at Fox Chase Cancer Center (2011 - 2025) evaluates the diagnostic performance of CMA and RNA fusion panels comprehensively. We also analyzed survival outcomes, co-mutations via NGS, and additional abnormalities (FISH, karyotype, FLT3) to elucidate *KMT2A*-PTD's prognostic and therapeutic implications, guiding optimal detection strategies and management in this high-mortality cohort.

Methods

This retrospective study identified specimens with confirmed *KMT2A* partial tandem duplication (PTD) from the Fox Chase Cancer Center molecular and cytogenetic database, spanning January 2011 to February 2025. Search criteria included specimens with *KMT2A*-PTD detection by chromosomal microarray analysis (CMA) and/or RNA fusion panels, with a concurrent diagnosis of myeloid neoplasm (acute myeloid leukemia [AML], myelodysplastic syndromes [MDS], or myeloproliferative neoplasms [MPN]) at the time of *KMT2A*-PTD detection. The study aimed to identify all cases diagnosed by both methods. Individuals younger than 18, those with non-myeloid neoplasms, or those with unconfirmed *KMT2A*-PTD were excluded from the analysis. Approximately 5,218 eligible specimens were analyzed using CMA (Affymetrix CytoScan HD, 2,696,168 markers) in the cytogenetic database, and 720 eligible specimens were analyzed using next-generation sequencing (NGS)-based targeted RNA sequencing (Illumina TruSight RNA Fusion 523-gene panel). Corresponding bone marrow and peripheral

blood specimens were verified in the pathology database to determine the total number of patients. Patients were grouped based on the diagnosis at the time of detection of *KMT2A*-PTD. To enable comparison between two methods, all available longitudinal specimens from the identified *KMT2A*-PTD positive patients were included in the analysis. Patient demographics and relevant clinical history, including original diagnosis, disease duration, mortality, and transplant status, were extracted from medical records. Additionally, data from concurrent NGS-based targeted DNA sequencing (275 gene panel), FISH, Karyotype, *FLT3* and *NPM1* studies were extracted to resolve discordant test results by CMA and RNA fusion analysis using a composite reference standard. Genomic coordinates from CMA reports and breakpoints from RNA fusion panels were verified using the UCSC Genome Browser (hg19 assembly), and ENST00000534358.1 transcript (GRCh37.p13, KMT2A-001; Chromosome 11: 118,436,492–118,526,832, forward strand) of *KMT2A* gene, to determine genomic coordinates, duplicated exons and introns, PTD size, and functional domains (e.g., CXXC, PHD, SET). *KMT2A*-PTD cases were classified as simple or complex *KMT2A*-PTD (**Table 1**) based on allelic state, copy number, and variant allele frequency (VAF%) using definitions adopted from Tsai et al. (2022)[8].

Table 1. Definition of Simple and Complex KMT2A-PTD Allelic States and Copy Number Variations (adopted from Tsai et al. (2022)).

Type	Allelic State	Copy Number	Example
Simple KMT2A-PTD	1 wild-type allele (1 copy of KMT2A) + 1 PTD allele (2 copies of PTD exons, 1 copy of non-PTD exons)	Net +1 copy gain of PTD exons (total 3 copies), 2 copies of non-PTD exons	Diploid cell with one PTD allele, typically mosaic (VAF <100%), no trisomy 11 or CN-LOH on 11q23.3
Complex KMT2A-PTD			
- Gain of 11q23.3	1 wild-type + 2 PTD alleles	+3 copy gain of PTD exons (5 copies), +1 copy gain of non-PTD exons (3 copies)	Trisomy 11 or multiple PTD alleles

- Double Gain of 11q23.3	1 wild-type + 3 PTD alleles	+5 copy gain of PTD exons (7 copies), +2 copy gain of non-PTD exons (4 copies)	Multiple PTD alleles or additional 11q23.3 gains
- CN-LOH	0 wild-type + 2 PTD alleles	+2 copy gain of PTD exons (4 copies), no gain of non-PTD exons (2 copies)	CN-LOH on 11q23.3
Log2 Ratio Calculation	For VAF (f), copy number = ($2 + f$), Log2 Ratio = ($\log_2((2 + f)/2)$)	Confirms copy number gain of PTD exons relative to diploid baseline	Used to quantify copy number changes in genomic analysis

Note: The Log2 Ratio calculation quantifies copy number gain of PTD exons based on VAF, enabling comparison to a diploid baseline for genomic analysis.

There is no universally accepted gold standard for detecting *KMT2A*-PTDs due to the technical limitations of individual methods. To enable comparison in this retrospective study, a composite reference standard (CRS) was developed to assign *KMT2A*-PTD status to the test results from CMA or RNA fusion analysis. The CRS integrated CMA, RNA fusion, clinical correlation, bone marrow morphology, and ancillary study findings to classify specimens as *KMT2A*-PTD-positive or negative.

Assigment for *KMT2A*-PTD+ status by CMA and/or RNA fusion analysis:

- **True Positive:** Confirmed *KMT2A*-PTD via CMA and RNA fusion analysis, along with clinical indicators of myeloid neoplasm or a previous *KMT2A*-PTD diagnosis.
- **True Negative:** Absence of *KMT2A*-PTD in both CMA and RNA fusion tests, without supporting clinical or ancillary test evidence.
- **Discordant Results:** Specimens with discordant CMA and RNA fusion results were resolved using aggregated results of ancillary test results (FISH, Karyotype, Targeted DNA-sequencing panel to infer *KMT2A*-PTD status of the positive test, in order to establish false positive and false negatives.

The diagnostic performance of CMA and RNA fusion was assessed by calculating the detection rate (proportion of positive results), stratified by test type and specimen source (bone marrow vs. peripheral blood). For dual-tested specimens, the agreement between CMA and RNA fusion was quantified using the proportion of concordant results. The concordance analysis assessed

the agreement between CMA and RNA Fusion, including overall concordance, *KMT2A*-PTD concordance, Cohen's Kappa for chance-corrected agreement for *KMT2A*-PTD classification, McNemar's test for asymmetry in discordant pairs. Survival analysis evaluated mortality rates and survival times across various subgroups, employing Kaplan-Meier curves, Log-Rank tests, and Fisher's Exact Test to identify significant differences. NGS analysis determined gene frequencies, co-occurrence patterns, and myeloid neoplasm gene prevalence.

Quantitative *KMT2A*-PTD expression was analyzed using total split reads and SR/C as continuous variables, with expression levels (High, Moderate, Low) as a categorical variable, and correlated with myeloid neoplasm mutations, CMA-abnormalities and clinical outcomes using Mann-Whitney U Test, Kruskal-Wallis Test, Spearman's rank correlation, Fisher's exact test and Log-Rank tests. Statistical analyses were conducted using R (v4.2.3, with packages 'stats' for non-paramteric tests, 'survival' for Kaplan-Meier and Log-Rank analyses and 'exact2x2' for Fisher's exact test.

Results

Patient demographics and Clinical Characteristics

The study identified 17 patients ((n=12), 5 female (n=5); median age 68 years, range 42–79) with KMT2A-PTD-positive myeloid neoplasms, comprising 11 AML (6 secondary [transformed from MDS or MPN], 5 de novo), 4 MDS (2 high grade), and 2 MPN (1 high grade) **(Table 2)**. Mortality occurred in 10 patients (58.82%; 8 males, 2 female), with a median time from *KMT2A*-PTD detection to death of 5.5 months (range 0.5–17), primarily due to failure to achieve complete remission (8/10) or relapse (2/10; relapse-free survival 7.5 months, range 6–9). Seven patients remained alive (41.18%; 4 males, 3 female), with a median survival of 19 months (range 4–62). Hematopoietic stem cell transplant (HSCT) was performed in 7 patients (41.18%), with 5 alive (71.43%) and 2 deceased (28.57%). Non-transplanted patients (10/17) had a higher mortality rate (8/10, 80%) compared to transplanted patients (2/7, 28.57%; Fisher's Exact Test,

p ≈ 0.0574). Median time from *KMT2A*-PTD detection to transplant was 5 months (range 3–8), with a median disease-free survival post-transplant of 12 months (range 8–53).

Table 2. Patients' clinical characteristics, mortality status and *KMT2A*-PTD status

Patient	Gender	Diagnosis at KMT2A-PTD	High-Grade	Transplant	Survival Status	Survival Time (Months)*	Cause of Death	Simple or Complex KMT2A-PTD
1	Male	AML	Yes	Yes	Alive	57 (censored)	N/A	Simple
2	Male	AML	Yes	No	Dead	6	Refractory AML	Complex
3	Male	AML	Yes	No	Dead	17	Relapse AML	Simple
4	Male	AML	Yes	Yes	Alive	51 (censored)	N/A	Simple
5	Male	AML	Yes	No	Dead	17	Complications + fall	Simple
6	Female	AML	Yes	No	Dead	2	Refractory AML	Simple
7	Male	AML	Yes	No	Dead	2	Induction failure	Simple
8	Male	High-grade MDS	Yes	No	Dead	6	Refractory	Simple
9	Male	AML	Yes	No	Dead	3	Refractory AML	Simple
10	Female	AML	Yes	Yes	Dead	14	Relapse AML	Complex
11	Male	High-grade MPN	Yes	Yes	Dead	13	Transplant toxicity	Simple

12	Male	MPN	No	Yes	Alive	19 (censored)	N/A	Simple
13	Female	High-grade MDS	Yes	Yes	Alive	15 (censored)	N/A	Simple
14	Male	AML	Yes	No	Dead	4	Refractory AML	Simple
15	Male	MDS	No	No	Alive	4 (censored)	N/A	Simple
16	Female	AML	Yes	Yes	Alive	13 (censored)	N/A	Non-canonical
17	Female	MDS	No	No	Alive	62 (censored)	N/A	Simple

Specimen characteristics

Of 97 specimens (79 bone marrow, 18 peripheral blood), 31 were KMT2A-PTD-positive, detected by CMA (24/31) and/or RNA fusion (21/22). *KMT2A*-PTD was classified as simple (14 patients: 2, 3, 4, 5, 6, 7, 8, 9, 11, 12, 13, 14, 15, 17), complex (2 patients: Patient 2 [trisomy 11, +2 copy gain] and Patient 10 [11q CN-LOH, +2 copy gain]), or non-canonical (1 patient: 16, exons 27–36) **(Table 1).**

Chromosomal Microarray Analysis

CMA confirms PTD in Patients 1, 2, 3, 8, 9, 10, 11, 12, 13, 14 (partial), 15, 17, with sizes (10,890–65,301 bp) overlapping RNA breakpoints. Patients 4–7 lack detection by CMA, but detected by RNA fusion panel, indicating cryptic PTDs. *KMT2A*-PTD Genomic coordinates reported by CMA (**Figure 1**) were mapped to the ENST00000534358.1 transcript (KMT2A-001; GRCh37.p13, hg19), confirming duplicated exons (e.g., 2–8, 2–10) (Figure 2) and functional domains (CXXC, PHD, SET) (**Supplemental Table 2**). The KMT2A-213 transcript (chromosome 11:118,307,205–118,397,539, GRCh38.p14, hg19) has 36 exons, with CMA coordinates aligning with exons 2–20 (except Case 16), affecting key oncogenic domains (CXXC, PHD, Bromodomain). Patient 16 showed an atypical *KMT2A*-PTD involving introns 26-27 to 35-36 and exons 27-36 (SET domain), outside the typical breakpoints in exons 2-11, raising questions about whether it can be considered a true PTD. *KMT2A*-PTDs involved

multiple functional domains. High-frequency region (Exons 2–5, Introns 1-2 to 4-5) was covered in 17 of 20 specimens, indicating a core region of *KMT2A*-PTDs affecting the CXXC domain (exons 4–5), critical for oncogenic activity in AML, MDS, and MPN. Mid-frequency region (Exons 6–8, Introns 6-7 to 8-9) invoved the PHD domain (exons 6–10) covered in 8 specimens (Patient 1, 2, 9, 11, 13, 14, 15, 17), and the AT Hooks (exons 1–2) in five cases (Patient 2, 3, 11, 15, 17). Involvement of the Bromodomain (exons 11–20) was observed in three cases (Patient 2, 14, 17). The degree of CXXC domain involvement varied, with partial involvement noted in five cases (Patient 1, 3, 8, 10, 13).

Figure 1. *KMT2A*-PTD Genomic coordinates detected by CMA with coverage of exons and introns of KMT*2A* gene (KMT2A-213, ENST00000534358.1 transcript, hg19).

Additional chromosomal abnormalities detected by Chromosomal microarray analysis

In seven patients (1, 3, 8, 12, 13, 15, 16), *KMT2A*-PTD was identified as the sole cytogenetic abnormality through chromosomal microarray analysis (CMA). Conversely, in four patients (4, 5, 6, 7), while CMA did not detect *KMT2A*-PTD, alternative aberrations were observed **(Figure 2; Supplemental Table 3).** These included numerical gains (trisomy/tetrasomy 13, trisomy 8), deletions (3q, 11p in Patient 6), and copy-neutral loss of heterozygosity (CN-LOH) at 11q (Patient 7). However, RNA fusion analysis subsequently revealed KMT2A-PTD in these four patients, suggesting a small duplication (~10–50 kb) at 11q23.3 (e.g., chr11:118,302,712-118,368,013) that was either below the detection limit of CMA or not present in the tested genomic DNA. *KMT2A*-PTD positive patients (2, 9, 10, 11, 14, 17) have 16 secondary abnormality types, compared to 6 in the *KMT2A*-PTD positive negative group (4, 5, 6, 7). The analytical focus for patients 4-7 had been on whole-chromosome gains or large deletions. Among the six patients positive for *KMT2A*-PTD by CMA (2, 9, 10, 11, 14, 17), all exhibited complex karyotypes. These complex karyotypes comprised the *KMT2A*-PTD alongside numerical abnormalities, such as trisomy 11 (Patient 2), trisomies 8 and 13 (Patient 10), and gains of 1q, 2p, 8, and 11p/q segments (Patients 14, 17). Structural abnormalities documented in these six patients included multi-chromosomal CN-LOH affecting 6q, 9p, 13q, 16p, 7q, 16q, and 11q (Patients 2, 9, 10, 11, 14), and losses of 6p and Yq (Patients 14, 17).

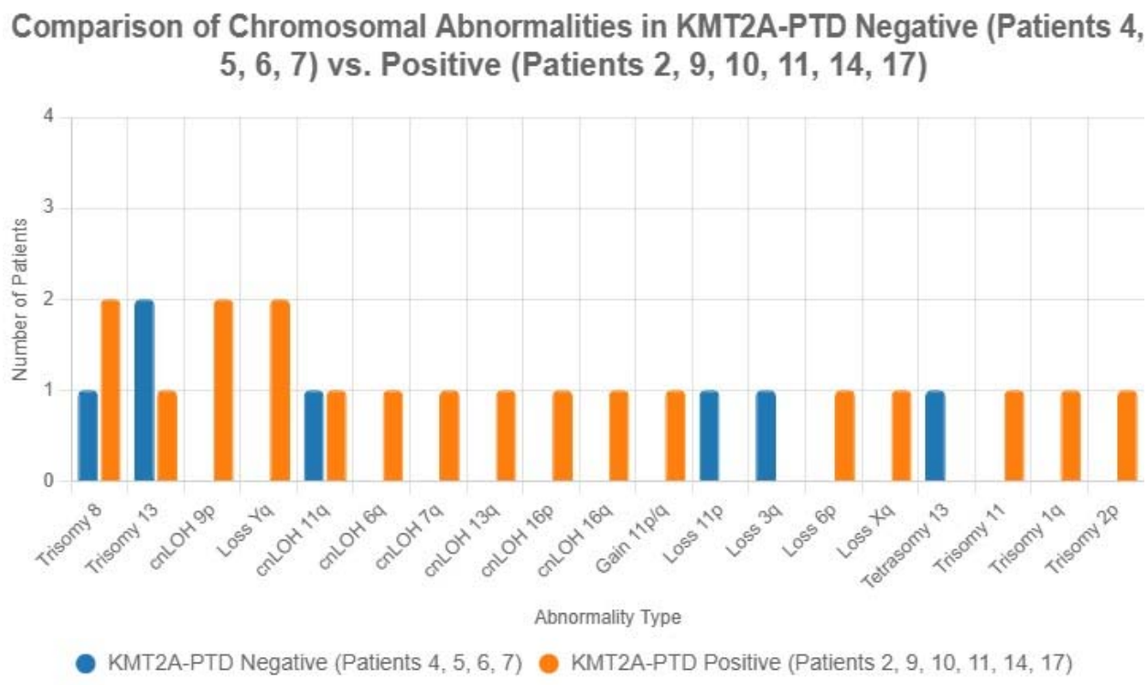

Figure 2. Comparison of Chromosomal Abnormalities in CMA KMT2A-PTD Negative vs Positive patients.

RNA fusion analysis

The RNA fusion panel confirms *KMT2A*-PTD in 21 specimens across 16 patients (Cases 1–15, 17). Patient 16 is excluded due to lack of RNA fusion analysis. The KMT2A-001 transcript (chromosome 11:118,307,205–118,397,539, hg19) comprises 36 exons. Breakpoints were identified in exon 2 (118,339,490–118,339,559), exon 10 (118,355,577–118,355,690), exon 11 (118,359,329–118,359,475), and exon 8 in Patient 17 (118,353,137–118,353,210) (**Figure 3; Supplemental Table 4)**. Common breakpoint patterns included exon 10 to exon 2 (16,200 bp, Patients 1, 2, 4, 5, 7, 13, 14, 15) and exon 11 to exon 2 (13,720 bp, Patients 3, 6, 8, 9, 10, 12). Variant breakpoints were exon 10 to exon 2 (15,539 bp, Patient 11) and exon 8 to exon 2 (19,985 bp, Patient 17). The size of the KMT2A partial tandem duplications ranged from 13,720 bp to 19,985 bp (Patient 17). Larger duplications may have a greater impact on protein function. The reading frame was in-frame in 19 of 21 specimens, potentially leading to HOX gene dysregulation. Out-of-frame duplications were observed in Patient 3-Specimen 2 and Patient 14-Specimen 2, which might be less oncogenic. The KMT2A protein's functional domains, including AT Hooks (exons 1–2), CXXC zinc finger (exons 4–5), PHD-finger (exons 6–10), Bromodomain (exons 11–20), and SET domain (exons 27–36), were generally retained. An exception was Patient 17, whose partial PHD-finger retained only 11%. With the exception of Patient 17's first

segment (containing the CXXC domain and 11% of the PHD-finger), all specimens retained the CXXC, F/Y-rich N/C-terminus, PHD-finger, and SET domains. The alteration in Patient 17 could affect chromatin interactions.

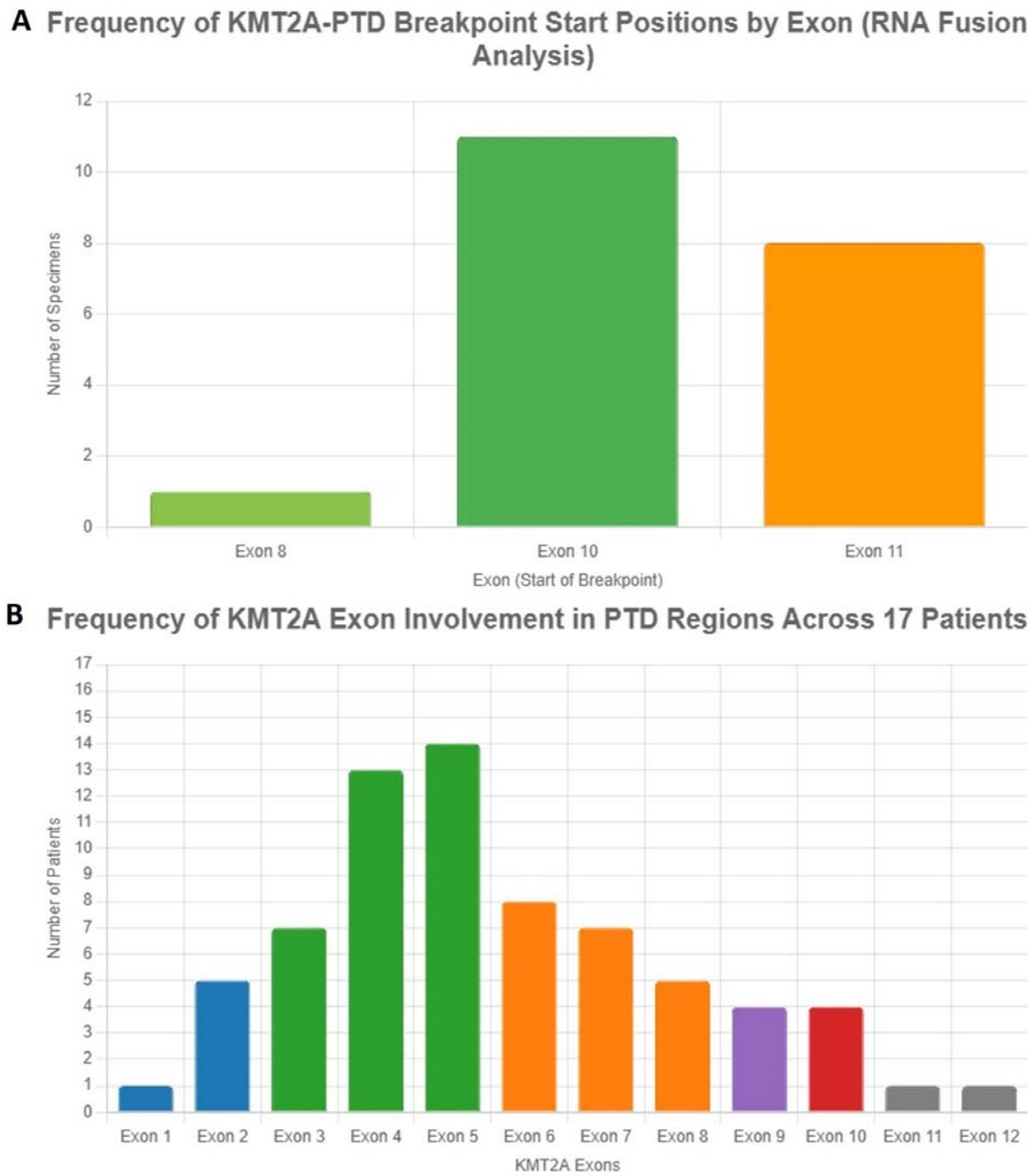

Figure 3. Frequency of Breakpoints and Exon involvement in PTD regions by RNA Fusion Results across 17 patients.

KMTA-PTD Expression Level Summary

RNA fusion split reads (1/2) represent sequencing reads spanning the fusion junction (e.g., exon 10 to exon 2), serving as a direct measure of *KMT2A*-PTD transcript presence. Higher split read counts indicate greater transcript abundance, reflecting quantitative expression. Based on split read counts (SR) and coverage (C), *KMT2A* partial tandem duplication expression levels were classified into high, moderate, and low categories (**Supplemental Table 5**). The high category included patients (1, 3, 4, 7, 8, 9, 10, and 12), showed median SR of 196 (range 102–365) and median SR/C of 0.1584 (range 0.1096–0.2032). The moderate category comprised patients (2, 3, 6, 10, and 13), exhibiting median SR of 95 (range 56–100) and median SR/C of 0.0998 (range 0.0609–0.1496). The low category consisted of patients 4, 5, 11, 14 (both specimens), 15, and 17, displaying median SR of 26.5 (range 3–48) and median SR/C of 0.0465 (range 0.0083–0.0884). RNA fusion analysis revealed significantly higher median split reads (102 vs 45.5, $p \approx 0.0423$) and SR/C ratio (0.1189 vs 0.0682, $p \approx 0.0387$) in *DNMT3A*-positive (n=10 patients, 13 specimens) compared to *DNMT3A*-negative (n=8 specimens) samples. High expression (Patients 1, 7, 8, 9, 12) correlates with high blast percentages and high-risk features (e.g., FLT3-ITD), while low expression (Patients 5, 11, 14, 15, 17) aligns with lower blasts or RNA-only PTDs **(Figure 4)**.

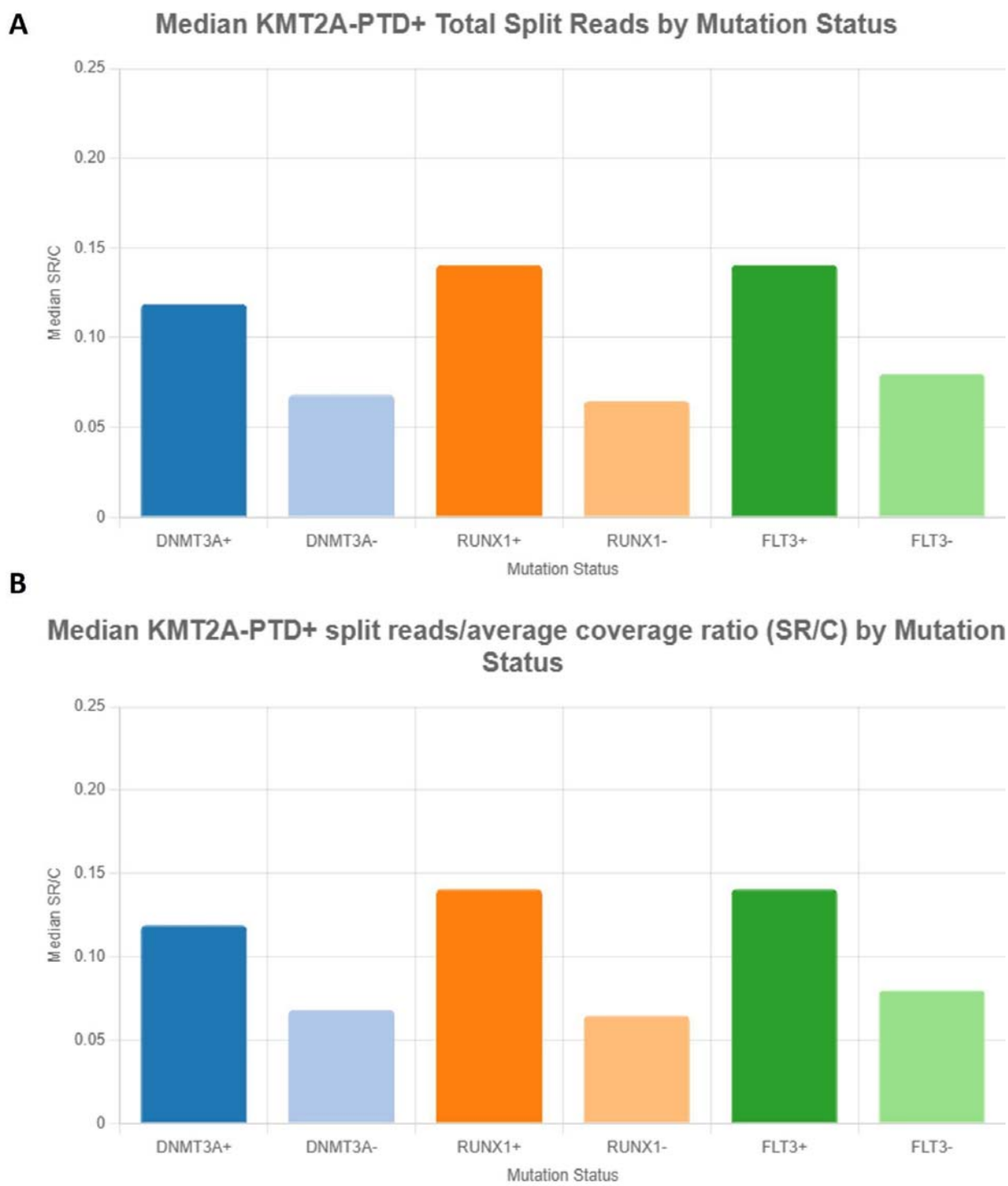

Figure 4. Median KMT2A-PTD+ Total Split Reads and Split Reads/Average Coverage (SR/C) by mutation status

Diagnostic Performance

CMA detected *KMT2A*-PTD in 24/31 specimens (sensitivity 77.42%), while RNA fusion detected 21/22 (sensitivity 95.45%). Overall concordance was 73.33% (κ=0.4667), with 45.16% *KMT2A-PTD* concordance. RNA fusion outperformed CMA in discordant cases (p=0.03516). FISH (22 specimens) showed *KMT2A* gain in 5 specimens (16.13% sensitivity), and karyotype (37 specimens) detected chromosome 11 gain in 7 (22.58% sensitivity). *FLT3* analysis (19 specimens) identified mutations in 9 (4 patients, 100% sensitivity for FLT3). This CRS approach

allowed for robust classification of *KMT2A*-PTD status by leveraging longitudinal data and clinical covariates, consistent with diagnostic study methodologies.

NGS Findings

Sixty specimens were analyzed for NGS-based targeted DNA sequencing (275-gene panel). DNMT3A was mutated in 31/60 (51.67%) specimens, TET2 in 18/60 (30.00%), and ASXL1 in 13/60 (21.67%). Among transcription factors, RUNX1 mutations were found in 25/60 (41.67%) and GATA2 in 9/60 (15.00%). Signaling pathway gene mutations included JAK2 in 15/60 (25.00%), FLT3 in 8/60 (13.33%), NRAS in 12/60 (20.00%), and PIK3CA in 7/60 (11.67%). Chromatin modifier mutations were noted in *EZH2* in 11/60 (18.33%) and KMT2A in 8/60 (13.33%) of the specimens.NGS of 59/97 specimens showed distinct mutational patterns in a 275-gene panel (n=60): *DNMT3A* (51.67%), *TET2* (30.00%), *ASXL1* (21.67%), *RUNX1* (41.67%), *GATA2* (15.00%), *JAK2* (25.00%), *FLT3* (13.33%), *NRAS* (20.00%), *PIK3CA* (11.67%), *EZH2* (18.33%), and *KMT2A* (13.33%). However, for the correlation with CMA and RNA fusion findings, only 32 *KMT2A*-PTD-positive specimens across 16 patients were considered and identified 92 unique genes. At the patient level, *DNMT3A* was mutated in 10/16 patients (62.5%), *RUNX1* in 8/16 (50%), *TET2* in 7/16 (43.75%), *NRAS* and *JAK2* in 4/16 (25% each), and WT1, ASXL1, ARID1A, and BCL6 in 3/16 (18.75% each). Specimen-level frequencies were DNMT3A (20/32, 62.5%), RUNX1 (14/32, 43.75%), *TET2* (10/32, 31.25%), and NRAS (8/32, 25%). Myeloid neoplasm genes dominated, with *DNMT3A, RUNX1,* and *TET2* reflecting epigenetic and transcriptional dysregulation. FLT3 mutations, although present in 4 patients, but detected by NGS in 1 patient (Patient 10, 5 specimens) and co-occurred with complex PTD, RUNX1T1 gain, and trisomy 8/13, indicating a high-risk profile. The *DNMT3A*-positive group included 10 patients (2, 3, 4, 6, 7, 8, 9, 10, 12, 13). A total of 13 specimens were *DNMT3A*-positive and 8 were *DNMT3A*-negative. Significantly higher median split reads were observed in *DNMT3A*-positive specimens (median: 102, range: 10–365) compared to *DNMT3A*-negative specimens (median: 45.5, range: 3–226) (Mann-Whitney U test, $p \approx 0.0423$). The median SR/C ratio was also significantly higher in *DNMT3A*-positive specimens (median: 0.1189, range: 0.0375–0.1888) compared to *DNMT3A*-negative specimens (median: 0.0682, range: 0.0083–0.1659) (Mann-Whitney U test, $p \approx 0.0387$). RNA fusion analysis revealed significantly higher median split reads (102 vs 45.5, $p \approx 0.0423$) of *KMT2A*-PTD and SR/C ratio

(0.1189 vs 0.0682, p ≈ 0.0387) in *DNMT3A*-positive (n=10 patients, 13 specimens) compared to *DNMT3A*-negative (n=8 specimens) samples. *RUNX1*-positive specimens (n=10) also showed a significantly higher median of total split reads (118, range 26–365) and median SR/C (0.1406, range 0.0799–0.1888) compared to *RUNX1*-negative samples (n=11) with a median of 43 (range 3–270) (p ≈ 0.0198) and (0.0646, range 0.0083–0.2032) (p ≈ 0.0234) for total split reads and median SR/C respectively.

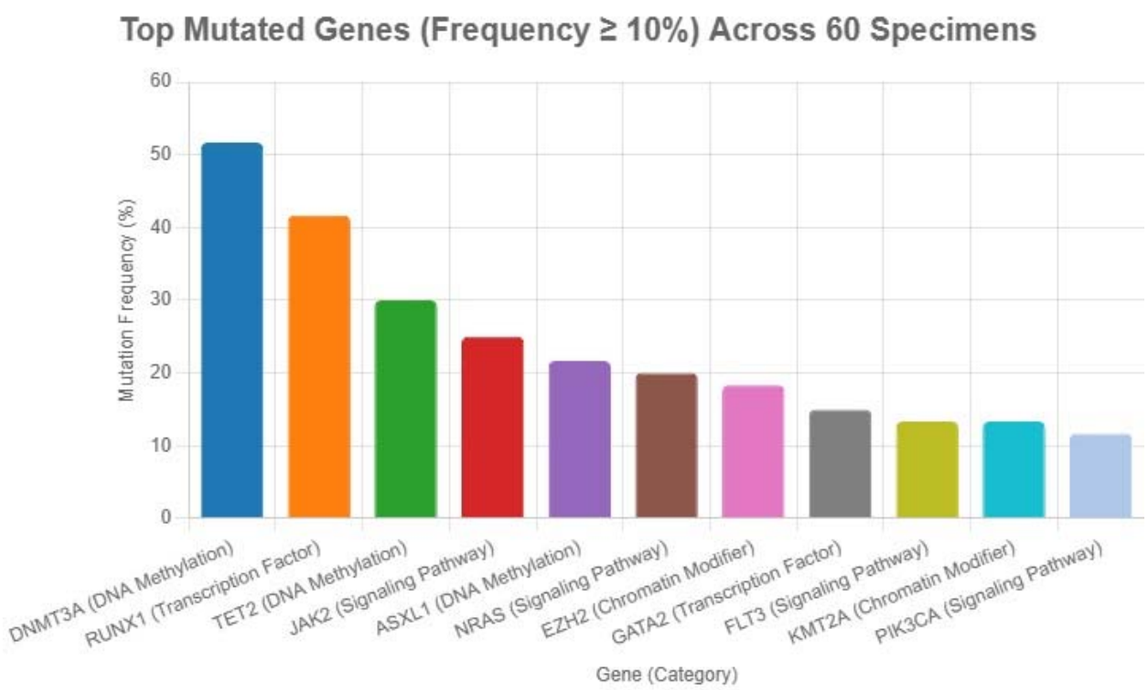

Figure 5. Top Mutated Genes across 60 Specimens analyzed by NGS-based targeted DNA sequencing (275-gene panel)

Survival Outcomes

Overall mortality was 58.82% (10/17), with 80% of deceased patients being male (8/10). FLT3-positive patients (3, 7, 9, 10) exhibited 100% mortality (median survival 8.5 months, range 2–

17), significantly worse than FLT3-negative patients (46.15% mortality, $p \approx 0.0456$, Log-Rank Test). Transplant significantly improved survival (28.57% mortality vs. 80% in non-transplanted, $p \approx 0.0367$, Log-Rank Test), with alive transplanted patients (e.g., Patient 4: 51 months) showing prolonged survival. Patients with *DNMT3A* mutations had a 60% mortality rate (median survival 8.5 months), *RUNX1* 62.5% (14 months), and *TET2* 42.86% (4 months). FLT3 mutation in Patient 10 correlated with 100% mortality (14 months), despite transplant. Abnormal karyotypes (8 patients), including trisomy 8 (Patients 3, 5, 10), +der(13;13) (Patient 4), and del(3)(q12q21) (Patient 6), showed 62.5% mortality (median 14 months), not significantly different from normal karyotypes (55.56%, $p \approx 0.8843$). FISH-detected KMT2A gains (4 patients) had 50% mortality ($p \approx 0.6287$), and RUNX1T1 gains (3 patients) had 100% mortality ($p \approx 0.0891$, marginally significant).

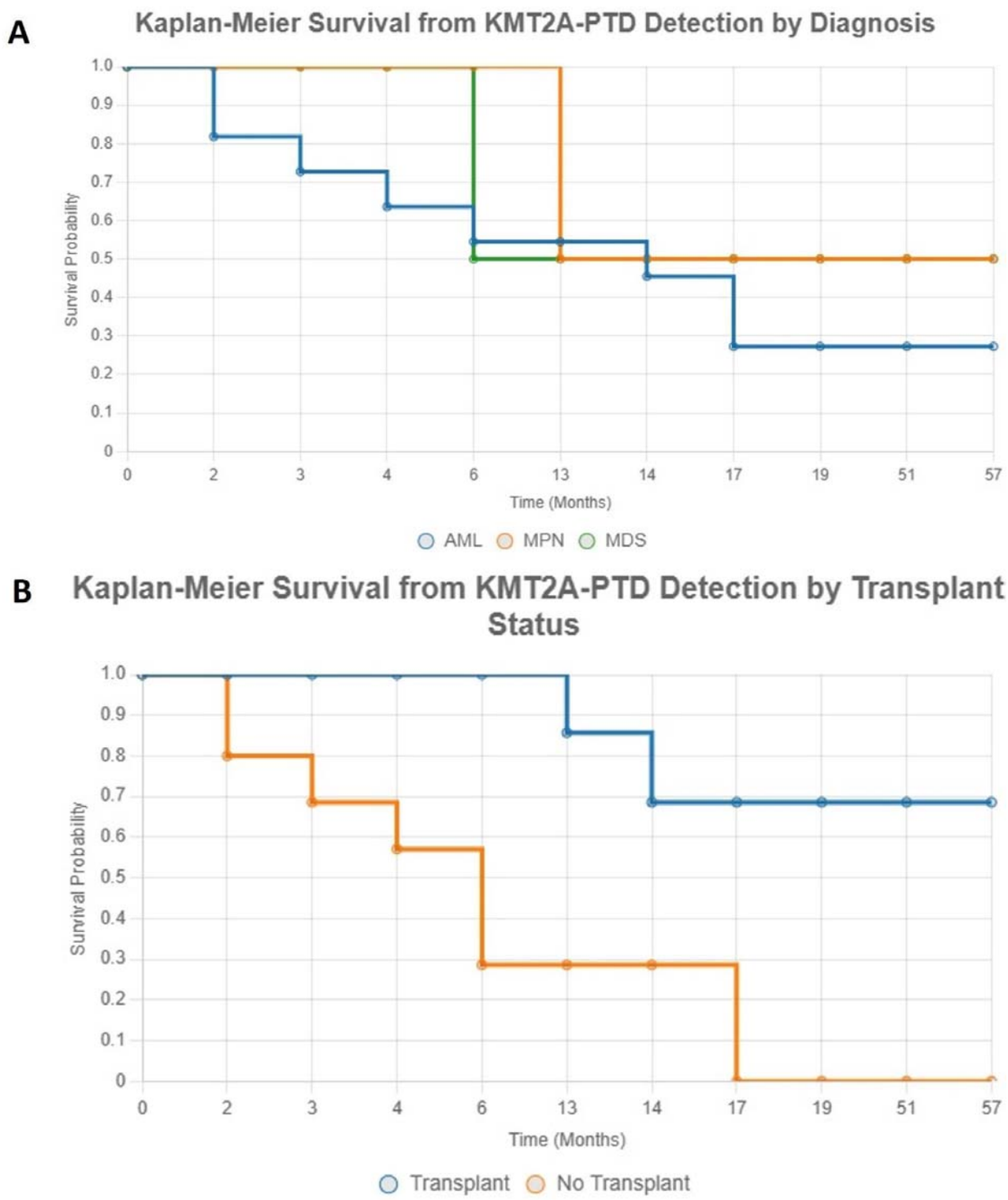

Figure 6. Kaplan-Meier Survival from KMT2A-PTD detection, based on the disease groups and transplant status.

Discussion

KMT2A is a large transcription factor (430 kD) similar to the Drosophila melanogaster trithorax (TRX) gene, containing AT-hook domains for DNA binding, a methyltransferase homology domain, and a SET domain[9]. Leukemogenesis can occur through *KMT2A* fusion with either a transcriptionally active partner gene or a partner that promotes dimerization of the KMT2A fragment, acting as a pro-leukemogenic factor[10]. *KMT2A*-PTD is thought to function similarly to the latter type of KMT2A translocations, involving dimerization. *KMT2A*-PTD, a structural variant spanning 10–50 kb, poses significant diagnostic challenges due to its size, which is below the resolution of karyotyping (5–10 Mb) and standard FISH *KMT2A* break-apart probes. These probes, designed for translocations, fail to reliably detect intragenic duplications due to signal overlap in interphase nuclei, as evidenced by Patient 16's non-canonical PTD (exons 27–36) showing only 9/200 cells with *KMT2A* gain[2]. In contrast, CMA detected *KMT2A*-PTD in approximately 50% of cells, aligning with a 40% blast count in bone marrow, indicating that the PTD was characteristic of the leukemic clone [7]**.** This discrepancy underscores CMA's superior sensitivity for copy number variations (CNVs) compared to FISH, which achieved only 16.13% sensitivity in this cohort [10]. Routine next-generation sequencing (NGS) panels, designed for short nucleotide variants, face limitations with intronic breakpoints, requiring custom bioinformatics pipelines to detect structural variants like *KMT2A*-PTD [5]. Despite the capability of NGS to identify PTD through split reads or CNV analysis, its reliance on high variant allele fraction (VAF >10%) reduces reliability in low-tumor-content samples, as observed in RNA-only *KMT2A*-PTD+ Patients 4 - 7 [11]**.** CMA, with dense SNP and copy number markers, excels at detecting CNVs and CN-LOH (e.g., 11q CN-LOH in Patient 10), but its 77.42% sensitivity misses cryptic PTDs without CNVs. RNA fusion panels, leveraging split-read analysis, achieve 95.45% sensitivity in tested specimens, detecting functional transcripts even in low-VAF clones, as in Patients 4–7, validated by NGS, morphology, karyotype, and FISH [3].

The overall concordance between CMA and RNA fusion was 73.33% (κ=0.4667), with a KMT2A-PTD-specific concordance of 45.16%, highlighting their complementary roles [12]. RNA fusion's superiority in discordant cases (McNemar's test, p=0.03516) reflects its ability to detect cryptic PTDs, while CMA's detection of non-canonical PTDs (e.g., Patient 16) and additional abnormalities (e.g., Patient 14's trisomy 8, cnLOH at 7q22.1qter) supports its utility in

comprehensive genomic profiling [13]**.** FISH and karyotyping, with sensitivities of 16.13% and 22.58%, respectively, served as supplementary tools, identifying high-risk features such as chromosome 11 gain in Patient 2 and *RUNX1T1* gain in Patients 7 and 10 [14]. FLT3 mutation analysis, achieving 100% sensitivity, was critical for prognosis, with all FLT3-positive patients (3, 7, 9, 10) died (Log-Rank Test, p=0.0456), consistent with AML's adverse risk profile[15] .

The KMT2A-PTD-positive group exhibited greater genomic complexity, with 17 secondary chromosomal abnormality types compared to 6 in the PTD-negative group, reflecting increased clonal heterogeneity [16]. Unique abnormalities in the positive group (Patients 2, 9, 10, 11, 14, 17) included cnLOH on 6q, 9p, 13q, 16p, 16q, and 7q, losses on Yq, 6p, and Xq, and gains on 1q, 2p, 11p/q, and trisomy 11, which may amplify oncogenic mutations (e.g., *JAK2*, *CDKN2A*, *EZH2*) and drive aggressive clonal evolution [17]. In contrast, the PTD-negative group (Patients 4, 5, 6, 7) showed fewer abnormalities, including unique loss of 11p, loss of 3q, and tetrasomy 13, suggesting distinct clonal drivers linked to RNA fusion detection of cryptic PTDs [18]. The PTD-negative group's abnormalities, such as cnLOH 11q encompassing ATM in Patient 7 and trisomy 13 associated with RUNX1/FLT3 mutations in Patients 4 and 5, align with AML's intermediate-to-poor prognostic profiles [19].

CMA-detected *KMT2A*-PTD correlates with a complex genomic landscape, characterized by gains (e.g., Trisomy 8, Trisomy 1q), losses (e.g., Loss Yq, Loss Xq), and copy-neutral events (e.g., cnLOH 9p, cnLOH 7q), indicating increased clonal heterogeneity or disease progression. In contrast, the negative group has fewer abnormalities, primarily trisomies (8, 13), tetrasomy 13, and specific losses (3q, 11p) or cnLOH (11q). The negative group shows clinical associations, such as cnLOH 11q encompassing *ATM* (Patient 7) and trisomy 13 linked to *RUNX1/FLT3* mutations (Patients 4, 5), aligning with AML risk profiles (Trisomy 8: intermediate-risk; Trisomy 13: poor prognosis).

The positive group's multi-chromosomal cnLOH (6q, 9p, 11q, 13q, 7q, 16q) drives allelic imbalance and oncogenic mutations (e.g., *JAK2*, *CDKN2A, EZH2*), suggesting aggressive clonal evolution. The negative group's focus on numerical gains (e.g., trisomy/tetrasomy 13) and deletions (3q, 11p) indicates distinct clonal drivers. RNA-only detection in Patients 4–7 suggests cryptic or low-VAF PTDs, supported by low read support. In the positive group, 11q alterations amplify KMT2A-PTD, absent in Patients 4–6, explaining CMA detection. Patient 7's cnLOH 11q (ATM) does not affect KMT2A-PTD detection by CMA.

NGS analysis revealed *DNMT3A* (62.5%), *RUNX1* (50%), and *TET2* (43.75%) as frequent co-mutations, reflecting *KMT2A*-PTD's synergy with epigenetic and transcriptional dysregulation [20]. The *KMT2A*-PTD/DNMT3A/FLT3-ITD combination, observed in Patients 3, 7, 9, and 10, is associated with poor prognosis and high relapse rates, as FLT3-ITD amplifies signaling dysregulation [21]. *DNMT3A* mutations, overlapping with trisomy 2p in Patient 14, and *EZH2* mutations, amplified by cnLOH 7q in the same patient, suggest a dosage effect enhancing leukemogenesis [22]. *RUNX1* mutations, coupled with trisomy 21 in Patient 14 and trisomy 13 in Patients 5 and 10, impair hematopoiesis and synergize with FLT3, driving AML progression [23]. FLT3 mutations, particularly in Patient 10, co-occurred with complex PTD, *RUNX1T1* gain, and trisomy 8/13, contributing to 100% mortality [24].

The high mortality rate (58.82%, median survival 5.5 months) underscores KMT2A-PTD's poor prognosis, particularly with complex PTD (Patients 2, 10) and FLT3 mutations [6]. Hematopoietic stem cell transplantation (HSCT) significantly improved survival (Log-Rank Test, p=0.0367), with 71.43% of transplanted patients alive (e.g., Patient 4: 51 months), though its efficacy was limited in FLT3-positive cases (e.g., Patient 10: 14 months) [25]. The study's small sample size (17 patients, 30 dual-tested specimens) limited statistical power, especially for FLT3 (n=4) and complex PTD (n=2) analyses [26]. Patient 16's non-canonical PTD, lacking RNA fusion confirmation, highlights the need for validation with reverse transcription polymerase chain reaction (RT-PCR) or optical genome mapping (OGM) [27]. Limited peripheral blood testing (7/97 specimens) biased results toward bone marrow clones, potentially underestimating circulating PTD clones [28].

In conclusion, CMA and RNA fusion are complementary for KMT2A-PTD detection, with RNA fusion excelling in identifying cryptic PTDs and CMA providing robust genomic profiling [29]. NGS, FISH, karyotype, and FLT3 analysis enhance risk stratification, guiding targeted therapies such as menin inhibitors for KMT2A-PTD and FLT3 inhibitors for FLT3-ITD-positive cases [30]. HSCT remains a critical intervention for improving outcomes in this high-mortality cohort, particularly in first complete remission [31]. Combined testing optimizes the management of KMT2A-PTD-positive myeloid neoplasms, addressing their complex genomic landscape and poor prognosis.

Authorship:

P.A and J.P. conceived the original idea for this study The diagnostic workup was. The literature review was performed by B.S. and J.P. Data collection and analysis were carried out by B.S and J.P. Data interpretation was performed by J.P., and B.S. B.S. wrote the original draft. Critical review and editing of the manuscript was undertaken by B.S., J.P., P.A., R.F., N.M., M.W, and R.N. All authors approved the final version of the manuscript for submission.

Acknowledgments:

The molecular, cytogenetic and clinical data being utilized in the study were collected previously as part of the patient's routine clinical care. No separate specimens were collected for the study. The Institutional Review Board of Fox Chase Cancer Center provided ethical approval for this work. All authors state that the presented material does not include any information, unique characteristics or identifiers that could be used alone or in combination with other information to identify, directly or indirectly, any patients of the study.

Conflict-of-interest disclosure: The authors declare no competing commercial interests.

Data availability

Deidentified raw CMA data (CEL files) and RNA sequencing data supporting the identification of *KMT2A*-Partial Tandem Duplications, along with a tab-separated values (TSV) file containing breakpoints, read support, and transcript annotations generated using Arriba, are available upon reasonable requests. This data can be obtained by contacting the corresponding author, Reza Nejati (Reza.Nejati@fccc.edu), subject to compliance with the Institutional Review Board (IRB) policies of Fox Chase Cancer Center to ensure patient confidentiality and ethical standards.

Supplemental Table 1: Comparison of Methodologies for KMT2A-PTD detection

Method	Description	Strengths	Limitations	Role in Detection	Detectability of KMT2A-PTD
RT-PCR (Gold Standard)	Uses primers to amplify specific KMT2A exon junctions (e.g., exon 8 → exon 2), followed by Sanger sequencing.	- High specificity and sensitivity for PTD junctions. - Detects low-VAF PTDs (<10%). - Confirms functional transcript. - Cost-effective, rapid. - Widely used in AML/MDS diagnostics.	- Requires known junction sites, - misses rare/non-canonical PTDs and complex structural variants. - RNA quality-dependent. - Single-target focus, misses other alterations.	Definitive confirmation of PTD junctions; validates CMA/RNA-seq findings.	**Simple**: Detectable (e.g., exon 8 → exon 2). **Complex**: Detectable (same junctions), but may need multiple primer sets for atypical cases.
Chromosomal Microarray (CMA)	High-resolution SNP arrays (e.g., Affymetrix CytoScan HD) detect CNVs and allelic imbalances via Log2 Ratio, BAF, and Allele Difference.	- High resolution (1,148 bp) detects small CNVs (10–50 kb) including cryptic KMT2A-PTD - Quantifies VAF (e.g., ~0.7). - Robust for genomic gains (e.g., Log2 Ratio ~0.4, BAF ~0.62).	- No transcript/junction confirmation. - May miss low-VAF or complex variants. - Requires transcript-based validation.	Initial screening for copy number gains; detects simple and complex PTDs.	**Simple**: Detectable (+1 copy gain of PTD exons). **Complex**: Detectable (+2, +3, or +5 copy gains, e.g., trisomy 11 case).
RNA Fusion Analysis (TruSight)	Targeted RNA-seq captures 523 cancer genes, including KMT2A, to detect fusion junctions via split reads/discordant pairs.	- Confirms functional transcripts (e.g., exon 8 → exon 2, VAF ~0.65). - High sensitivity for expressed fusions. - Screens for other fusions.	- RNA quality-dependent. -Misses DNA-level KMT2A-PTD -Fails to detect due to transcriptional silencing - False negatives due to algorithm sensitivity or intronic breakpoints. - Limited to targeted genes.	Transcript-level confirmation; complements CMA.	**Simple**: Detectable (junction-specific). **Complex**: Detectable, but non-standard junctions may be missed.

Multiplex Ligation-dependent Probe Amplification (MLPA)	Uses exon-specific probes (e.g., KMT2A exon 4) to detect copy number changes.	- Simple, cost-effective. - Detects exon-specific gains.	- Limited probe coverage (e.g., exon 4 only). - No junction/transcript data. - Lower resolution than CMA/NGS. - Misses PTDs not involving exon 4 (e.g., case 32).	Targeted screening for specific exons; less comprehensive.	**Simple**: Partially detectable (if probes cover PTD exons). **Complex**: Partially detectable, misses non-targeted exons.
Next-Generation Sequencing (General, e.g., WGS/WES)	Includes whole-genome sequencing (WGS), whole-exome sequencing (WES), or broad panels to detect structural variants or fusions.	- WGS maps genomic breakpoints. - WES/RNA-NGS detects junctions. - Quantifies VAF and co-mutations (e.g., FLT3-ITD). - Comprehensive profiling.	- Expensive, computationally intensive. - WES may miss intronic breakpoints. - Requires high-quality DNA/RNA and advanced bioinformatics.	Comprehensive genomic/transcriptomic profiling; research or complex cases.	**Simple**: Detectable (breakpoints or junctions). **Complex**: Detectable, especially with WGS or RNA-NGS.
Hybrid Capture NGS (Heme-NGS)	Custom hybrid-capture NGS panel targets entire KMT2A coding sequence; detects PTD via exon coverage ratios (e.g., exons 1–10 vs. 27/36) with z-score >2.	- Covers entire KMT2A coding region, detects canonical and **atypical PTDs (e.g., single-exon PTDs).** - Analytical sensitivity 3–5% VAF for variants, 10% for PTDs. - Detects co-occurring mutations (e.g., FLT3, DNMT3A). - Uniform coverage improves PTD detection vs. amplicon-based NGS.	- False positives from cryptic structural variants. - Limited by short-read sequencing for SVs. - Requires >100× coverage. - Interfered by 11q23.3 SVs. - Less precise for PTD copy number vs. OGM.	Comprehensive molecular profiling; detects PTDs and co-mutations in AML standard-of-care.	**Simple**: Detectable (z-score >2 for exons 1–10). **Complex**: Detectable, but may misidentify copy number (e.g., case 36 vs. case 15).

Optical Genome Mapping (OGM)	High-resolution imaging of long DNA molecules to detect structural variants using CTTAAG labels (~6 kb spacing).	- Resolves complex SVs (e.g., 5 kb+ duplications). - Detects PTD copy number (e.g., 2–4 copies, cases 9, 15, 20, 36). - Agnostic, no gene-specific probes. - VAF as low as 5%.	- Not widely available. - No transcript confirmation. - Limited exon-level resolution (e.g., only 4 labels in KMT2A). - Expensive, specialized equipment.	Structural variant detection; resolves complex PTDs and mimics.	**Simple**: Detectable (structural duplication). **Complex**: Detectable, with precise copy number estimation.
Fluorescence In Situ Hybridization (FISH)	Uses fluorescent probes to detect DNA sequences or structural alterations on chromosomes.	- Detects large amplifications or numerical changes (e.g., trisomy 11). - Clinically routine for KMT2A translocations.	- Standard KMT2A probes target translocations, not PTDs. - Small PTD size (~10–50 kb) below resolution. - Custom probes needed.	Detects trisomy 11 or large 11q amplifications, not PTD directly.	**Simple**: Not detectable (too small). **Complex**: Potentially detectable if large 11q23.3 amplification (>100 kb); not for CN-LOH or small PTD.
Karyotype	Visualizes chromosomes to identify numerical or gross structural abnormalities.	- Detects numerical changes (e.g., trisomy 11). - Routine in AML/MDS diagnostics.	- Resolution (5–10 Mb) cannot detect PTD (~10–50 kb). - No allelic or transcript data.	Detects trisomy 11, not PTD.	**Simple**: Not detectable (too small). **Complex**: Detectable only for trisomy 11 or large amplifications (>5–10 Mb); not for CN-LOH or focal PTD.

Supplemental Table 2: KMT2A-PTD Genomic Coordinates, Exon Coverage, and Functional Domains detected by CMA (Affymetrix CytoScan HD)

Patient	Coordinates (hg19, 11q23.3)	Size (bp)	High-Grade	Exons Covered (Fully/Partially)	Introns Covered (Fully/Partially)	Functional Domains Affected
1	118,338,294–118,354,329	16,035	Yes (AML)	2, 3, 4, 5, 6, 7, 8 (full)	1-2 (partial), 2-3, 3-4, 4-5, 5-6, 6-7, 7-8 (full), 8-9 (partial)	CXXC (partial), PHD
2	118,302,712–118,368,013	65,301	Yes (AML)	1, 2, 3, 4, 5, 6, 7, 8, 9, 10, 11, 12, 13, 14, 15, 16, 17, 18, 19, 20 (full)	1-2, 2-3, 3-4, 4-5, 5-6, 6-7, 7-8, 8-9, 9-10, 10-11, 11-12, 12-13, 13-14, 14-15, 15-16, 16-17, 17-18, 18-19, 19-20 (full), 20-21 (partial)	AT Hooks (partial), CXXC, PHD, Bromodomain
3	118,316,622–118,350,109	33,487	Yes (AML)	2, 3, 4, 5 (full)	1-2 (partial), 2-3, 3-4, 4-5 (full), 5-6 (partial)	AT Hooks (partial), CXXC
3	118,338,856–118,350,013	11,157	Yes (AML)	2, 3, 4, 5 (full)	1-2 (partial), 2-3, 3-4, 4-5 (full), 5-6 (partial)	CXXC (partial)
8	118,339,219–118,350,109	10,890	Yes (MDS)	2, 3, 4, 5 (full)	1-2 (partial), 2-3, 3-4, 4-5 (full), 5-6 (partial)	CXXC (partial)
9	118,338,217–118,355,553	17,336	Yes (AML)	2, 3, 4, 5, 6, 7, 8, 9 (full)	1-2 (partial), 2-3, 3-4, 4-5, 5-6, 6-7, 7-8, 8-9 (full), 9-10 (partial)	CXXC, PHD
10	118,329,464–118,350,109	20,645	Yes (AML)	2, 3, 4, 5 (full)	1-2 (partial), 2-3, 3-4, 4-5 (full), 5-6 (partial)	CXXC
10	118,329,613–118,350,110	20,497	Yes (AML)	2, 3, 4, 5 (full)	1-2 (partial), 2-3, 3-4, 4-5 (full), 5-6 (partial)	CXXC
10	118,338,218–118,350,028	11,810	Yes (AML)	2, 3, 4, 5 (full)	1-2 (partial), 2-3, 3-4, 4-5 (full), 5-6 (partial)	CXXC (partial)
11	118,315,622–118,359,052	43,430	Yes (MPN)	2, 3, 4, 5, 6, 7, 8, 9, 10 (full)	1-2 (partial), 2-3, 3-4, 4-5, 5-6, 6-7, 7-8, 8-9, 9-10 (full), 10-11 (partial)	AT Hooks, CXXC, PHD

11	118,315,329–118,350,110	34,781	Yes (MPN)	2, 3, 4, 5 (full)	1-2 (partial), 2-3, 3-4, 4-5 (full), 5-6 (partial)	AT Hooks, CXXC
12	118,337,944–118,350,110	12,166	No (MPN)	2, 3, 4, 5 (full)	1-2 (partial), 2-3, 3-4, 4-5 (full), 5-6 (partial)	CXXC
12	118,338,218–118,350,110	11,892	No (MPN)	2, 3, 4, 5 (full)	1-2 (partial), 2-3, 3-4, 4-5 (full), 5-6 (partial)	CXXC
13	118,335,186–118,354,898	19,712	Yes (MDS)	2, 3, 4, 5, 6, 7, 8 (full)	1-2 (partial), 2-3, 3-4, 4-5, 5-6, 6-7, 7-8, 8-9 (full)	CXXC (partial), PHD
14	118,331,660–118,365,263	33,603	Yes (AML)	2, 3, 4, 5, 6, 7, 8, 9, 10, 11, 12, 13, 14, 15, 16, 17 (full)	1-2 (partial), 2-3, 3-4, 4-5, 5-6, 6-7, 7-8, 8-9, 9-10, 10-11, 11-12, 12-13, 13-14, 14-15, 15-16, 16-17 (full), 17-18 (partial)	CXXC, PHD, Bromodomain
15	118,315,623–118,355,769	40,146	No (MDS)	2, 3, 4, 5, 6, 7, 8, 9, 10 (full)	1-2 (partial), 2-3, 3-4, 4-5, 5-6, 6-7, 7-8, 8-9, 9-10 (full), 10-11 (partial)	AT Hooks (partial), CXXC, PHD
16	118,374,566–118,425,419	50,853	Yes (AML)	27, 28, 29, 30, 31, 32, 33, 34, 35, 36 (full)	26-27 (partial), 27-28, 28-29, 29-30, 30-31, 31-32, 32-33, 33-34, 34-35, 35-36 (full)	None (non-canonical)
17	118,315,433–118,368,014	52,581	No (MDS)	2, 3, 4, 5, 6, 7, 8, 9, 10, 11, 12, 13, 14, 15, 16, 17, 18, 19, 20 (full)	1-2 (partial), 2-3, 3-4, 4-5, 5-6, 6-7, 7-8, 8-9, 9-10, 10-11, 11-12, 12-13, 13-14, 14-15, 15-16, 16-17, 17-18, 18-19, 19-20 (full), 20-21 (partial)	AT Hooks, CXXC, PHD, Bromodomain

Supplemental Table 3. Unique Chromosomal Abnormalities (CMA), Frequency, Coordinates, Genes, and Mortality Status

Abnormality Type	Frequency (Patients)	Genomic Coordinates (hg19)	Copy Number	Genes Involved	Affected Patients	Mortality Status
KMT2A-PTD (11q23.3 gain)	7	11q23.3 (e.g., 118,302,712–118,368,013; 118,315,329–118,359,052)	3	KMT2A	2, 9, 10, 11, 14, 17	2, 9, 10, 11, 14 (Deceased); 17 (Alive)
cnLOH 6q	1	6q11.1q12 (61,968,745–69,384,530)	2 hmz	None noted	2	Deceased
cnLOH 9p	2	9p24.3p21.3 (192,128–22,067,830); 9p24.3p13.2 (192,129–36,530,875)	2 hmz	JAK2 (9p24.1)	2, 11	Deceased
cnLOH 16p	1	16p13.3p12.1 (1–27,692,222)	2 hmz	CREBBP (16p13.3)	2	Deceased
Trisomy 11	1	(11)x3	3	KMT2A, ATM	2	Deceased
Tetrasomy 13	1	(13)x4	4	FLT3 (13q12.2), RUNX1 (21q22.12)	4	Alive
Trisomy 8	3	(8)x3	3	MYC (8q24.21)	5, 14	5, 14 (Deceased)
Trisomy 13	2	(13)x3	3	FLT3, RUNX1	5, 10	5, 10 (Deceased)
Loss 3q	1	3q13.12q22.3 (107,030,100–136,985,329)	1	None noted	6	Deceased

Loss 11p	1	11p13 (32,133,120–33,004,788; 33,655,491–36,757,347)	1	WT1 (11p13)	6	Deceased
cnLOH 11q	2	11q13.1q25 (65,896,397–134,942,626); 11q13.1q23.3 (65,271,647–118,329,463)	2 hmz	ATM (11q22.3), KMT2A (11q23.3)	7, 10	7, 10 (Deceased)
cnLOH 13q	1	13q12.11q34 (19,911,441–115,067,322)	2 hmz	FLT3, RUNX1	9	Deceased
Trisomy 2	1	(2)x3	3	None noted	14	Deceased
Loss 9	1	(9)x1	1	JAK2	14	Deceased
Loss 12	1	(12)x1	1	None noted	14	Deceased
Trisomy 21	1	(21)x3	3	RUNX1	14	Deceased
Trisomy 1q	1	(1q)x3	3	None noted	14	Deceased
Trisomy 2p	1	(2p)x3	3	None noted	14	Deceased
cnLOH 7q	2	7q22.1q36.3 (100,850,659–159,119,220; 100,528,675–159,119,220)	2 hmz	EZH2 (7q36.1)	14	Deceased
Trisomy 13q	1	13q21.33q34 (68,948,880–115,073,823)	3	FLT3, RUNX1	14	Deceased
cnLOH 16q	1	(16q)x2 hmz	2 hmz	CBFB (16q22.1)	14	Deceased
Loss Yq	1	(Yq)x0	0	None noted	14	Deceased
Loss 6p	1	6p25.3p22.3 (1–19,893,817)	1	None noted	17	Alive

Gain 11p/q	1	11p15.5p11.2 (198,510–48,116,232); 11p11.2q13.5 (48,116,233–76,944,946); 11q13.5q25 (76,944,947–134,891,125)	3	KMT2A, ATM	17	Alive

Supplemental Table 4: KMT2A-PTD RNA Fusion Panel Results: Breakpoints, Exons, Size, Reading Frame and Retained Domains

Patient	Diagnosis	Breakpoints	Exons	Size (bp)	Reading Frame	Retained Domains
Patient 1	AML (45% blasts)	11:118,355,690 to 11:118,339,490	Exon 10 to Exon 2	16,200	In-frame	CXXC zinc finger (100%), F/Y-rich N/C-terminus (100%), PHD-finger (100%), SET domain (100%)
Patient 2	De novo MPN	11:118,355,690 to 11:118,339,490	Exon 10 to Exon 2	16,200	In-frame	CXXC zinc finger (100%), F/Y-rich N/C-terminus (100%), PHD-finger (100%), SET domain (100%)
Patient 3	AML-MRC (50% blasts)	11:118,353,210 to 11:118,339,490	Exon 11 to Exon 2	13,720	In-frame	CXXC zinc finger (100%), F/Y-rich N/C-terminus (100%), PHD-finger (100%), SET domain (100%)
Patient 3	Inadequate for morphologic evaluation	11:118,353,210 to 11:118,339,490	Exon 11 to Exon 2	13,720	Out-of-frame	CXXC zinc finger (100%), F/Y-rich N/C-terminus (100%), PHD-finger (100%), SET domain (100%)
Patient 4	AML (45% blasts)	11:118,355,690 to 11:118,339,490	Exon 10 to Exon 2	16,200	In-frame	CXXC zinc finger (100%), F/Y-rich N/C-terminus (100%), PHD-finger (100%), SET domain (100%)
Patient 4	MDS (12% blasts)	11:118,355,690 to 11:118,339,490	Exon 10 to Exon 2	16,200	In-frame	CXXC zinc finger (100%), F/Y-rich N/C-terminus (100%), PHD-finger (100%), SET domain (100%)
Patient 4	MDS (12% blasts)	11:118,355,690 to 11:118,339,490	Exon 10 to Exon 2	16,200	In-frame	CXXC zinc finger (100%), F/Y-rich N/C-terminus (100%), PHD-finger (100%), SET domain (100%)
Patient 5	AML (80% blasts)	11:118,355,690 to 11:118,339,490	Exon 10 to Exon 2	16,200	In-frame	CXXC zinc finger (100%), F/Y-rich N/C-terminus (100%), PHD-finger (100%), SET domain (100%)

Patient 6	**Therapy-related AML (77% blasts)**	**11:118,353,210 to 11:118,339,490**	**Exon 11 to Exon 2**	**13,720**	**In-frame**	**CXXC zinc finger (100%), F/Y-rich N/C-terminus (100%), PHD-finger (100%), SET domain (100%)**
Patient 7	**AML with KMT2A-PTD (85% blasts)**	**11:118,355,690 to 11:118,339,490**	**Exon 10 to Exon 2**	**16,200**	**In-frame**	**CXXC zinc finger (100%), F/Y-rich N/C-terminus (100%), PHD-finger (100%), SET domain (100%)**
Patient 8	**RAEB-II**	**11:118,353,210 to 11:118,339,490**	**Exon 11 to Exon 2**	**13,720**	**In-frame**	**CXXC zinc finger (100%), F/Y-rich N/C-terminus (100%), PHD-finger (100%), SET domain (100%)**
Patient 9	**AML (85% blasts)**	**11:118,353,210 to 11:118,339,490**	**Exon 11 to Exon 2**	**13,720**	**In-frame**	**CXXC zinc finger (100%), F/Y-rich N/C-terminus (100%), PHD-finger (100%), SET domain (100%)**
Patient 10	**AML (92% blasts)**	**11:118,353,210 to 11:118,339,490**	**Exon 11 to Exon 2**	**13,720**	**In-frame**	**CXXC zinc finger (100%), F/Y-rich N/C-terminus (100%), PHD-finger (100%), SET domain (100%)**
Patient 10	**AML (85% blasts)**	**11:118,353,210 to 11:118,339,490**	**Exon 11 to Exon 2**	**13,720**	**In-frame**	**CXXC zinc finger (100%), F/Y-rich N/C-terminus (100%), PHD-finger (100%), SET domain (100%)**
Patient 11	**De novo MPN**	**11:118,355,029 to 11:118,339,490**	**Exon 10 to Exon 2**	**15,539**	**In-frame**	**CXXC zinc finger (100%), F/Y-rich N/C-terminus (100%), PHD-finger (100%), SET domain (100%)**
Patient 12	**De novo MPN**	**11:118,353,210 to 11:118,339,490**	**Exon 11 to Exon 2**	**13,720**	**In-frame**	**CXXC zinc finger (100%), F/Y-rich N/C-terminus (100%), PHD-finger (100%), SET domain (100%)**
Patient 13	**AML**	**11:118,355,690 to 11:118,339,490**	**Exon 10 to Exon 2**	**16,200**	**In-frame**	**CXXC zinc finger (100%), F/Y-rich N/C-terminus (100%), PHD-finger (100%), SET domain (100%)**

Patient 14	**AML**	**11:118,355,690 to 11:118,339,490**	**Exon 10 to Exon 2**	**16,200**	**In-frame**	**CXXC zinc finger (100%), F/Y-rich N/C-terminus (100%), PHD-finger (100%), SET domain (100%)**
Patient 14	**AML**	**11:118,355,690 to 11:118,339,490**	**Exon 10 to Exon 2**	**16,200**	**Out-of-frame**	**CXXC zinc finger (100%), F/Y-rich N/C-terminus (100%), PHD-finger (100%), SET domain (100%)**
Patient 15	**AML**	**11:118,355,690 to 11:118,339,490**	**Exon 10 to Exon 2**	**16,200**	**In-frame**	**CXXC zinc finger (100%), F/Y-rich N/C-terminus (100%), PHD-finger (100%), SET domain (100%)**
Patient 17	**AML**	**11:118,359,475 to 11:118,339,490**	**Exon 8 to Exon 2**	**19,985**	**In-frame**	**CXXC zinc finger (100%), PHD-finger (11%) in first segment; CXXC zinc finger (100%), F/Y-rich N/C-terminus (100%), PHD-finger (100%), SET domain (100%) in second segment**

Supplemental Table: 5 KMT2A-PTD RNA Fusion Panel Results (Arriba): Breakpoints, Split Reads, Discordant Mates, Coverage and Retained Domains

Patient	Specimen ID	Breakpoints	Reading Frame	Split Reads (1/2)	Discordant Mates	Coverage (1/2)	Notable Fusion Parameters
Patient 1	Bone Marrow	11:118,355,690 to 11:118,339,490	In-frame	143/127	118	1336/1321	High read support, robust coverage, no mismatches, duplicates not specified.
Patient 2	Bone Marrow	11:118,355,690 to 11:118,339,490	In-frame	54/46	51	880/1124	High read support, duplicates(29), mismatches(1).
Patient 3	Bone Marrow	11:118,353,210 to 11:118,339,490	In-frame	118/94	84	1920/930	High read support, robust coverage, duplicates(92).
Patient 3	Bone Marrow	11:118,353,210 to 11:118,339,490	Out-of-frame	17/39	23	1221/617	Low read support, out-of-frame fusion, duplicates(28), mismatches(2).
Patient 4	Bone Marrow	11:118,355,690 to 11:118,339,490	In-frame	46/56	55	963/752	High read support, duplicates(43), mismatches(2).
Patient 4	Bone Marrow	11:118,355,690 to 11:118,339,490	In-frame	20/21	18	492/436	Low read support, duplicates(24), reduced coverage.
Patient 4	Bone Marrow	11:118,355,690 to 11:118,339,490	In-frame	10/12	12	488/535	Very low read support, duplicates(15), mismatches(1).
Patient 5	Bone Marrow	11:118,355,690 to 11:118,339,490	In-frame	26/22	23	788/414	Moderate read support, duplicates(23), mismatches(1).

Patient 6	Bone Marrow	11:118,353,210 to 11:118,339,490	In-frame	27/34	23	1252/505	Moderate read support, high coverage, duplicates(24).
Patient 7	Bone Marrow	11:118,355,690 to 11:118,339,490	In-frame	68/68	63	941/837	High read support, duplicates(39), FLT3-ITD detected (medium confidence, breakpoints: 13:28608227 to 13:28608289, in-frame).
Patient 8	Bone Marrow	11:118,353,210 to 11:118,339,490	In-frame	83/97	75	1207/946	High read support, duplicates(65), low_entropy(20), mismatches(7).
Patient 9	Bone Marrow	11:118,353,210 to 11:118,339,490	In-frame	176/189	89	2434/1432	Very high read support, robust coverage, duplicates(141), FLT3-ITD detected (medium confidence, breakpoints: 13:28608234 to 13:28608312, in-frame).
Patient 10	(Peripheral Blood	11:118,353,210 to 11:118,339,490	In-frame	75/36	24	1139/537	High read support, duplicates(60), mismatches(2).
Patient 10	Bone Marrow	11:118,353,210 to 11:118,339,490	In-frame	58/37	15	885/385	Moderate read support, duplicates(46).
Patient 11	Bone Marrow	11:118,355,029 to 11:118,339,490	In-frame	3/10	5	184/279	Very low read support, duplicates(8), limited coverage.
Patient 12	Peripheral Blood	11:118,353,210 to 11:118,339,490	In-frame	123/103	71	1771/953	High read support, duplicates(181), low_entropy(23), mismatches(3).
Patient 13	Bone Marrow	11:118,355,690 to 11:118,339,490	In-frame	30/28	33	628/430	Moderate read support, duplicates(30), mismatches(1).

Patient 14	Bone Marrow	11:118,355,690 to 11:118,339,490	In-frame	10/3	4	485/209	Very low read support, duplicates(16), limited coverage.
Patient 14	Peripheral Blood	11:118,355,690 to 11:118,339,490	Out-of-frame	2/1	1	295/428	Extremely low read support, out-of-frame fusion, duplicates(5), transcript_id2 differs (ENST00000533790.1).
Patient 15	Bone Marrow	11:118,355,690 to 11:118,339,490	In-frame	18/13	17	710/530	Low read support, duplicates(12), mismatches(2).
Patient 17	Bone Marrow	11:118,359,475 to 11:118,339,490	In-frame	28/15	7	700/369	Low read support, unique exon 8 breakpoint, partial PHD-finger retention (11%), duplicates(60), low_entropy(1), mismatches(3).

Reference list

1. Strout, M.P., et al., *The partial tandem duplication of ALL1 (MLL) is consistently generated by Alu-mediated homologous recombination in acute myeloid leukemia.* Proc Natl Acad Sci U S A, 1998. **95**(5): p. 2390-5.
2. Seto, A., et al., *Genomic Characterization of Partial Tandem Duplication Involving the KMT2A Gene in Adult Acute Myeloid Leukemia.* Cancers (Basel), 2024. **16**(9).
3. Kao, H.W., et al., *High frequency of additional gene mutations in acute myeloid leukemia with MLL partial tandem duplication: DNMT3A mutation is associated with poor prognosis.* Oncotarget, 2015. **6**(32): p. 33217-25.
4. Choi, S.M., et al., *Partial tandem duplication of KMT2A (MLL) may predict a subset of myelodysplastic syndrome with unique characteristics and poor outcome.* Haematologica, 2018. **103**(3): p. e131-e134.
5. Dai, B., et al., *The Application of Targeted RNA Sequencing for KMT2A-Partial Tandem Duplication Identification and Integrated Analysis of Molecular Characterization in Acute Myeloid Leukemia.* J Mol Diagn, 2021. **23**(11): p. 1478-1490.
6. Shiah, H.S., et al., *Clinical and biological implications of partial tandem duplication of the MLL gene in acute myeloid leukemia without chromosomal abnormalities at 11q23.* Leukemia, 2002. **16**(2): p. 196-202.
7. Wei, Q., et al., *Detection of KMT2A Partial Tandem Duplication by Optical Genome Mapping in Myeloid Neoplasms: Associated Cytogenetics, Gene Mutations, Treatment Responses, and Patient Outcomes.* Cancers (Basel), 2024. **16**(24).
8. Tsai, H.K., et al., *Allelic complexity of KMT2A partial tandem duplications in acute myeloid leukemia and myelodysplastic syndromes.* Blood Advances, 2022. **6**(14): p. 4236-4240.
9. Meyer, C., et al., *The KMT2A/MLL consensus gene structure: a comprehensive update for research and diagnostic implications.* Leukemia, 2024. **38**(6): p. 1403-1406.
10. Basecke, J., et al., *The MLL partial tandem duplication in acute myeloid leukaemia.* Br J Haematol, 2006. **135**(4): p. 438-49.
11. Sun, Q.Y., et al., *Ordering of mutations in acute myeloid leukemia with partial tandem duplication of MLL (MLL-PTD).* Leukemia, 2017. **31**(1): p. 1-10.
12. Steudel, C., et al., *Comparative analysis of MLL partial tandem duplication and FLT3 internal tandem duplication mutations in 956 adult patients with acute myeloid leukemia.* Genes Chromosomes Cancer, 2003. **37**(3): p. 237-51.

13. Dorrance, A.M., et al., *Mll partial tandem duplication induces aberrant Hox expression in vivo via specific epigenetic alterations.* J Clin Invest, 2006. **116**(10): p. 2707-16.

14. Shin, S.Y., et al., *Chromosome 8 pentasomy with partial tandem duplication of 11q23 in a case of de novo acute myeloid leukemia.* Cancer Genet Cytogenet, 2009. **194**(1): p. 44-7.

15. Zorko, N.A., et al., *Mll partial tandem duplication and Flt3 internal tandem duplication in a double knock-in mouse recapitulates features of counterpart human acute myeloid leukemias.* Blood, 2012. **120**(5): p. 1130-6.

16. Zhang, Y., et al., *Stress hematopoiesis reveals abnormal control of self-renewal, lineage bias, and myeloid differentiation in Mll partial tandem duplication (Mll-PTD) hematopoietic stem/progenitor cells.* Blood, 2012. **120**(5): p. 1118-29.

17. Ariyama, Y., et al., *Amplification on double-minute chromosomes and partial-tandem duplication of the MLL gene in leukemic cells of a patient with acute myelogenous leukemia.* Genes Chromosomes Cancer, 1998. **23**(3): p. 267-72.

18. Ghasemian Sorbeni, F., et al., *Partial tandem duplication of KMT2A gene in patient afflicted with hypereosinophilic syndrome: A case report.* Cancer Genet, 2022. **268-269**: p. 111-114.

19. Kong, J., et al., *The initial level of MLL-partial tandem duplication affects the clinical outcomes in patients with acute myeloid leukemia.* Leuk Lymphoma, 2018. **59**(4): p. 967-972.

20. Whitman, S.P., et al., *DNA hypermethylation and epigenetic silencing of the tumor suppressor gene, SLC5A8, in acute myeloid leukemia with the MLL partial tandem duplication.* Blood, 2008. **112**(5): p. 2013-6.

21. Antherieu, G., et al., *Allogenic Stem Cell Transplantation Abrogates Negative Impact on Outcome of AML Patients with KMT2A Partial Tandem Duplication.* Cancers (Basel), 2021. **13**(9).

22. Mims, A.S., et al., *A novel regimen for relapsed/refractory adult acute myeloid leukemia using a KMT2A partial tandem duplication targeted therapy: results of phase 1 study NCI 8485.* Haematologica, 2018. **103**(6): p. 982-987.

23. Liu, H.C., et al., *Expression of HOXB genes is significantly different in acute myeloid leukemia with a partial tandem duplication of MLL vs. a MLL translocation: a cross-laboratory study.* Cancer Genet, 2011. **204**(5): p. 252-9.

24. Kawamura, M., et al., *Mutations of GATA1, FLT3, MLL-partial tandem duplication, NRAS, and RUNX1 genes are not found in a 7-year-old Down syndrome patient with*

acute myeloid leukemia (FAB-M2) having a good prognosis. Cancer Genet Cytogenet, 2008. **180**(1): p. 74-8.

25. Whitman, S.P., et al., *Long-term disease-free survivors with cytogenetically normal acute myeloid leukemia and MLL partial tandem duplication: a Cancer and Leukemia Group B study.* Blood, 2007. **109**(12): p. 5164-7.
26. He, Y., et al., *Expression of partial tandem duplication of mixed lineage leukaemia in patients with acute leukaemia and their relatives.* Chin Med J (Engl), 2014. **127**(2): p. 284-9.
27. Hayashi, M., et al., *Establishment of a novel childhood acute myeloid leukaemia cell line, KOPM-88, containing partial tandem duplication of the MLL gene and an in vivo model for childhood acute myeloid leukaemia using NOD/SCID mice.* Br J Haematol, 2007. **137**(3): p. 221-32.
28. Satake, N., et al., *Minimal residual disease in acute monocytic leukemia patient with trisomy 11 and partial tandem duplication of MLL.* Cancer Genet Cytogenet, 1997. **96**(1): p. 26-9.
29. Dorrance, A.M., et al., *The Mll partial tandem duplication: differential, tissue-specific activity in the presence or absence of the wild-type allele.* Blood, 2008. **112**(6): p. 2508-11.
30. Yamamoto, S., et al., *Partial tandem duplication of MLL gene in acute myeloid leukemia with translocation (11;17)(q23;q12-21).* Am J Hematol, 2005. **80**(1): p. 46-9.
31. Whitman, S.P., et al., *The MLL partial tandem duplication: evidence for recessive gain-of-function in acute myeloid leukemia identifies a novel patient subgroup for molecular-targeted therapy.* Blood, 2005. **106**(1): p. 345-52.